Coupling effects in proton scattering from ^{40}Ca

Journal Item

PHYSICAL REVIEW C **85**, 064603 (2012)

Coupling effects in proton scattering from ^{40}Ca

R. S. Mackintosh*
Department of Physical Sciences, The Open University, Milton Keynes, MK7 6AA, UK

N. Keeley
National Centre for Nuclear Research, ul. Andrzeja Sołtana 7, 05-400 Otwock, Poland

(Received 17 April 2012; published 1 June 2012)

Recent studies showed that neutron pickup makes a substantial contribution to the proton optical model potential (OMP) for light, mostly halo, target nuclei. Here, we extend those studies to a more "normal" target nucleus: ^{40}Ca. We present coupled reaction channel (CRC) calculations with the coupling of 30.3 MeV incident protons to deuterons and up to 12 states of ^{39}Ca. The proton elastic scattering S matrix from the CRC calculation is subject to $S_{lj} \rightarrow V(r) + \mathbf{l}\cdot\mathbf{s}\ V_{\rm SO}(r)$ inversion and the bare potential of the CRC calculation is subtracted, directly yielding a local and L-independent representation of the dynamic polarization potential (DPP). This is appropriate for comparison with phenomenological OMPs and local OMPs derived in local density folding models. The real-central part of the DPP is repulsive and cannot be represented as a uniform normalization of the bare potential, changing the rms radius. A series of model calculations reveal the dependence of the DPP on a range of parameters illuminating (i) departures of nucleon potentials of specific nuclei from global properties, (ii) the generation of repulsion, and (iii) the requirements for all-order CRC and deuteron breakup. Light is thrown on the nonlocality of the underlying DPP.

DOI: 10.1103/PhysRevC.85.064603 PACS number(s): 25.40.Cm, 24.10.Ht, 24.10.Eq, 25.40.Hs

I. INTRODUCTION

In earlier work [1–4] we evaluated, for light target nuclei, the contribution to the nucleon-nucleus optical model potential (OMP) of coupling to the deuteron channels through neutron pickup. It was uncertain whether the substantial contribution was particular to halo target nuclei [2–4] or perhaps just light nuclei [1]. Because of the importance of understanding the nucleon OMP, and because the contributions we found showed characteristic features of nonlocality and possible L dependence that could not easily be represented within a local density model, it is important to explore the contribution of pickup to the proton OMP for heavier target nuclei.

What we informally called "the contribution of pickup coupling to the proton OMP" is the dynamical polarization potential (DPP) induced in the proton-nucleus interaction by the coupling between the elastic proton channel and the deuteron channels defined by the pickup of neutrons leading to specific states of ^{39}Ca in this case. The formal DPP is discussed in Ref. [2] together with a comparison of various means of determining a local representation of it. In that reference we also give a full account of the procedure used in this work, the coupled channel (CC) plus inversion method, together with an account of its advantages and limitations. Briefly, this method involves a CC calculation [our usage of "CC" includes coupled reaction channel (CRC) and continuum-discretized coupled channel (CDCC)] followed by inversion of the resulting elastic scattering S matrix S_{lj} to obtain a single channel potential $V(r) + \mathbf{l}\cdot\mathbf{s}\ V_{\rm SO}(r)$ that reproduces the CC elastic scattering S matrix. The $S_{lj} \rightarrow V(r) + \mathbf{l}\cdot\mathbf{s}\ V_{\rm SO}(r)$ inversion is carried out using the iterative-perturbative (IP) procedure [5,6]. Subtracting the diagonal potential of the CC calculation (hereafter the "bare potential") from this inverted potential yields a local and L-independent representation of the DPP due to the coupling. We distinguish this local-equivalent DPP from the nonlocal and L-dependent formal DPP, and some of the consequences of the underlying nonlocality will be presented in what follows. It is worth emphasizing that this nonlocality is in no way related to the knock-on exchange nonlocality that is responsible for most of the energy dependence of the phenomenological nucleon OMP. Its effects on direct reactions can therefore not be assumed to be accounted for by the usual Perey [7] correction (see also Refs. [8,9]). Moreover, the L dependence is not related to the parity dependence that follows from certain other exchange processes.

Among the issues raised by Ref. [2] in the discussion of the DPP is the question of double counting between the deuteron channels and the nonorthogonal particle-hole excitations that are included in current theories of the OMP. There are two points to be made concerning this. The first is that an essential role is played by the deuteron that is propagating in potentials that have density gradients around the nucleus; this leads to L-dependent and nonlocal properties of the underlying DPP (of which we determine the local equivalent). Such properties cannot be represented in current theories which involve a local-density approximation, and some of the properties of the DPP, such as the repulsive nature of the real part, seem to be a result of these finite-nucleus effects. At the end of the paper, we comment on the relationship between the present work and modern folding model theories. The second point is that theories of the OMP essentially relate to global properties whereas the calculations described here open up the possibility of determining "shell corrections" to such global properties since the DPPs can be related directly to the l, j, and binding energy of the neutron that is picked up. An example is the shell

*r.mackintosh@open.ac.uk

effect on the phenomenological spin-orbit term presented by Sakaguchi *et al* [10]. We shall make an attempt to explore these two points through various model calculations that we describe below.

The real part of the DPP turns out to be such that it cannot be represented as a uniform renormalization of the bare potential: it modifies the rms radius of the real potential significantly. It is also almost always repulsive, and this raises the question of why this should be so and why the other properties should be the way they are. In other words, are the conclusions intelligible in qualitative terms? Related to this is the question of how these processes contribute to the nuclide-by-nuclide departure of phenomenological potentials from global potentials, a question which is surely relevant to the extrapolation of global potentials away from the valley of stability. These questions have led us to carry out a series of model calculations in order to get some purchase on these problems. However, we do not claim to provide anything like definitive answers to these questions, although we do claim to show a practical way of exploring them.

Throughout this work, nuclear potentials are characterized with volume integrals J normalized and defined following Satchler [11]. Consistently with our previous papers, we adopt the convention that attractive or absorptive potentials have volume integrals J with a positive sign, so J is effectively minus the volume integral. The subscripts R, IM, RSO, and IMSO identify real-central, imaginary-central, real-spin-orbit (real-SO) and imaginary-SO components. Units of MeV fm^3 are understood throughout. Potentials plotted in the figures have the natural convention that attractive potentials or DPPs are negative. Throughout, "L dependence" refers to the dependence of the OMP or DPP on the orbital angular momentum of the projectile and "l dependence" refers to dependence of the DPP on the orbital angular momentum of the transferred nucleon within the nucleus.

An outline of this paper is as follows: In Sec. II we specify the details of the CRC calculations. In Sec. III we present the results in four categories: in Sec. III A we present the DPP for a standard set of pickup states, together and individually, with a standard set of OMP parameters and spectroscopic factors; in Sec. III B model calculations illuminate the dependence of the DPP for coupling to the ^{39}Ca ground state on the OMP and other factors; in Sec. III C we study the dependence of the DPP upon j transfer, Q value etc.; in Sec. III D we compare second-order and full CRC calculations. In Sec. IV we summarize the findings and their significance and discuss the questions raised for future work.

II. THE CRC CALCULATIONS

All CRC calculations to be described below were performed with the code FRESCO [12]. The deuteron D state was included and there was a full finite-range description of the reaction channel coupling. Nonorthogonality corrections were included.

States of ^{39}Ca included. The full set of states of ^{39}Ca in the deuteron channels involved in the calculations described below were: (i) $3/2^+$ ground state (g.s.), (ii) $1/2^+$ at 2.467 MeV; (iii) $7/2^-$ at 2.796 MeV; (iv) $5/2^+$ at 5.6175 MeV; $5/2^+$ at 7.3148 MeV; $5/2^+$ at 8.5148 MeV. Note that the $5/2^+$ pickup strength is actually spread over 9 principal states. Apart from one calculation, the calculations that did include all the $5/2^+$ strength lumped these nine states into three states at 5.6175, 7.3148 and 8.5148 MeV, having the same aggregate pickup strength. The choice of states in ^{39}Ca was as in our previous reanalysis [13] of the ^{40}Ca(d, t) data of Doll *et al*. [14], where we omitted states with spectroscopic factors $C^2S < 0.2$ in order to keep the number of states within tractable limits while retaining the main coupling strength.

Bare potentials. The nucleon potential that gives the best fit to the elastic scattering angular distribution (AD) and analyzing power (AP) will, of course, depend upon what deuteron channel states are included. The nucleon potential used in all calculations (except as specifically noted) was that given in the "$\sigma + p$" column in Table II of Ref. [15]. This potential has $J_{\rm R} = 408.55$ MeV fm^3, $J_{\rm IM} = 109.28$ MeV fm^3, and $J_{\rm RSO} = 9.3055$ MeV fm^3, with zero imaginary spin-orbit potential. The rms radius of the real-central potential is 4.1130 fm

TABLE I. For protons scattering from ^{40}Ca at 30.3 MeV/nucleon, volume integrals ΔJ (in MeV fm^3) of the four components of the DPP induced by (p,d) coupling. The $\Delta R_{\rm rms}$ column gives the change of rms radius of the real-central component (in fm). The two final columns present, respectively, the change in the total reaction cross section induced by the coupling, and the integrated cross section to the specific coupled reaction channels. Note that negative $\Delta J_{\rm R}$ corresponds to repulsion. The excitation energies of the states, in MeV, are given in parentheses.

States coupled	$\Delta J_{\rm R}$	$\Delta J_{\rm IM}$	$\Delta J_{\rm RSO}$	$\Delta J_{\rm IMSO}$	$\Delta R_{\rm rms}$	Δ(Reac CS) (mb)	State CS (mb)
$3/2^+$ (0.0)	−12.53	14.64	0.8605	−0.3257	0.0344	52.47	7.93
$1/2^+$ (2.467)	−4.00	5.62	0.2224	0.0894	0.0088	25.77	6.51
$5/2^+$ (5.6175)	−3.36	10.35	0.5100	0.3339	0.0206	39.26	4.95
$5/2^+$ (7.3148)	−0.75	3.58	0.1918	0.0964	0.0071	15.33	1.61
$5/2^+$ (8.5148)	−0.4	2.99	0.1697	0.0712	0.0058	13.26	1.15
$7/2^-$ (2.796)	+0.42	1.29	0.118	0.0083	0.0018	6.3	0.889
All ($3 \times 5/2^+$)	−18.48	27.29	1.4265	−0.5630	0.0492	93.07	17.3
Sum	−20.62	38.47	2.0724	0.2735	0.0785	152.39	23.0
All ($9\times 5/2^+$)	−16.18	25.48	1.2615	−0.5686	0.0442	88.27	17.8
Linearity test	+3.66	−0.74	−0.462	−0.2544	−0.0079	−2.13	26.6

and, with no coupling, the total reaction cross section (CS) is 925.03 mb. We shall see how the corresponding values of all these quantities differ for the potentials determined by inversion. We shall justify the use of this potential for our study of the pickup DPP when we discuss the linearity test in Sec. III A. The deuteron potential was based on the standard Watanabe folding model with the proton and neutron potentials given by the Koning-Delaroche [16] global potential and with the deuteron described as in our previous works [1–4].

Breakup of the deuteron. In most of these calculations we do not include the breakup of the outgoing deuteron for two reasons: (i) It proves to be less important than it is for light target nuclei [2–4], and (ii) it greatly increases the computer time, precluding the possibility of complete parameter searches to optimize the fits with the full CRC calculations. Nevertheless, we do present some results in which breakup is included. The breakup calculations were similar to those described in our previous work (see, e.g., Refs. [1–4]). The $n + p$ continuum was discretized in momentum space into bins of width $\Delta k = 0.125$ fm^{-1} up to a maximum value $k_{\max} = 0.5$ fm^{-1}, corresponding to a deuteron "excitation energy" of 12.7 MeV.

III. RESULTS OF *S*-MATRIX INVERSION

A. Dynamical polarization potential with standard parameters

Table I presents characteristic properties of the DPP for various pickup channels and with the standard (Hnizdo [15]) parameters and no deuteron breakup (BU). The three $5/2^+$ states are weighted mean states representing the pickup strength of nine $5/2^+$ states. The line "All $(3 \times 5/2^+)$" represents the DPP due to the first group of 6 states $(3/2^+, \ldots, 7/2^-)$ coupled simultaneously. The line marked "Sum" presents the numerical sum of the DPP characteristics for the same 6 channels coupled independently; we explain below the rationale for presenting this. The line marked "All $(9 \times 5/2^+)$" presents the DPP characteristics for all states coupled simultaneously with the 9 individual $5/2^+$ states included separately. In all cases, there is no mutual coupling between pickup channels. The line "Linearity test" is discussed below.

The characteristics of the DPP are presented in terms of the changes in the volume integral, ΔJ, of specific components of the p-^{40}Ca potential. These are obtained by subtracting the volume integrals of the bare potential components from those of the potential obtained by inversion of the elastic scattering S_{lj} as calculated by FRESCO. In addition, $\Delta R_{\rm rms}$ is the change in the rms radius of the real-central component that is induced by the reaction channel coupling. Table I presents "Δ(Reac CS)," the change in total reaction cross section due to the coupling, and "State CS," the integrated cross section to the particular coupled pickup channel or channels. We include the sum of $\Delta R_{\rm rms}$ values, although there is no reason why these should add; likewise for Δ(Reac CS).

It is interesting to see that, for cases where the DPP is very small, "Δ(Reac CS)," the increase in total reaction cross section, is by no means proportionately small. This is one reflection of the fact that the DPP is a higher-order effect.

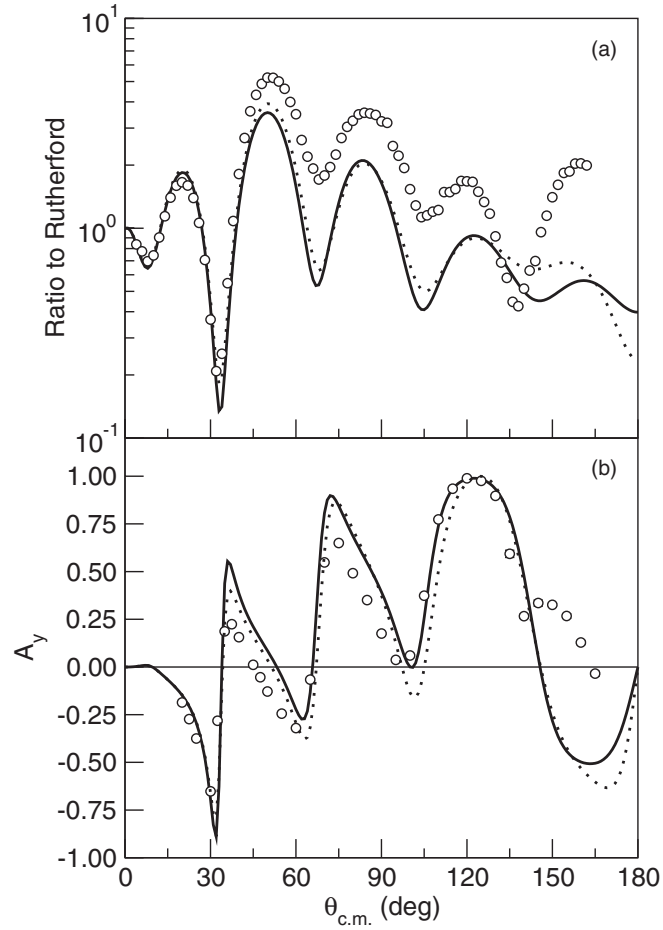

FIG. 1. For 30.3 MeV protons scattering from ^{40}Ca, the AD (a) and AP (b) for the case "All $(3 \times 5/2^+)$" in Table I compared with the measured values. The dotted line presents "UD" calculations for the same case, as described in Sec. III D.

It is satisfying to note that the imaginary SO DPP has opposite signs for coupling to $3/2^+$ and $5/2^+$ states and is relatively small for coupling to the $l = 0$ state. The very small DPP generated by coupling to the $7/2^-$ has an *attractive* real-central part, contrary to all the other cases.

The effect on the angular distribution and analyzing power of the coupling of all the states is large: in Fig. 1 we compare the observables resulting from the full calculation in which the $5/2^+$ strength is lumped in three states, see line "All $(3 \times 5/2^+)$" in Table I. The fit without coupling is quite good except at backward angles, as can be seen in Fig. 2 where we present the AD and AP calculated with the bare potential [15] with no coupling. We return to this figure when we discuss the linearity test below.

In Fig. 3 we compare the actual DPPs for the "All $(3 \times 5/2^+)$" case (three lumped $5/2^+$ states) with the DPP calculated with all nine $5/2^+$ states of ^{39}Ca coupled to the proton channel. The agreement is rather close for the larger, central, components. All further calculations that include $5/2^+$ coupling involve the three lumped states; this is essential for parameter searches with full coupling. Note that the repulsion in the real-central DPP is largest at the nuclear center. This

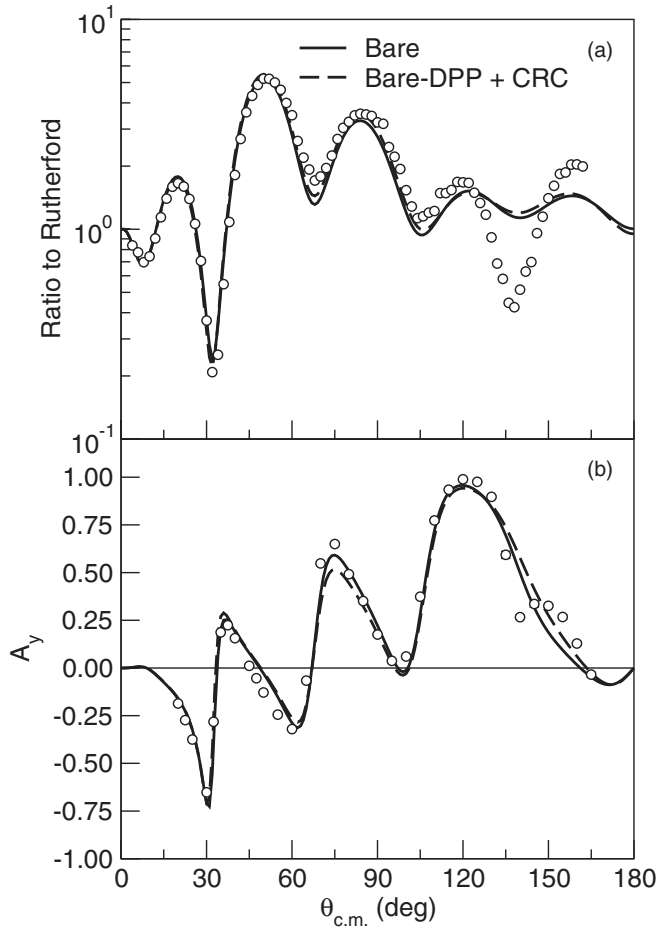

FIG. 2. For 30.3 MeV protons scattering from ^{40}Ca, the AD (a) and AP (b) for the "All $(3 \times 5/2^+)$" CRC calculation involving a modified bare potential in which the DPP has been subtracted from the original bare potential of Ref. [15], compared with a no-coupling calculation using the bare potential of Ref. [15].

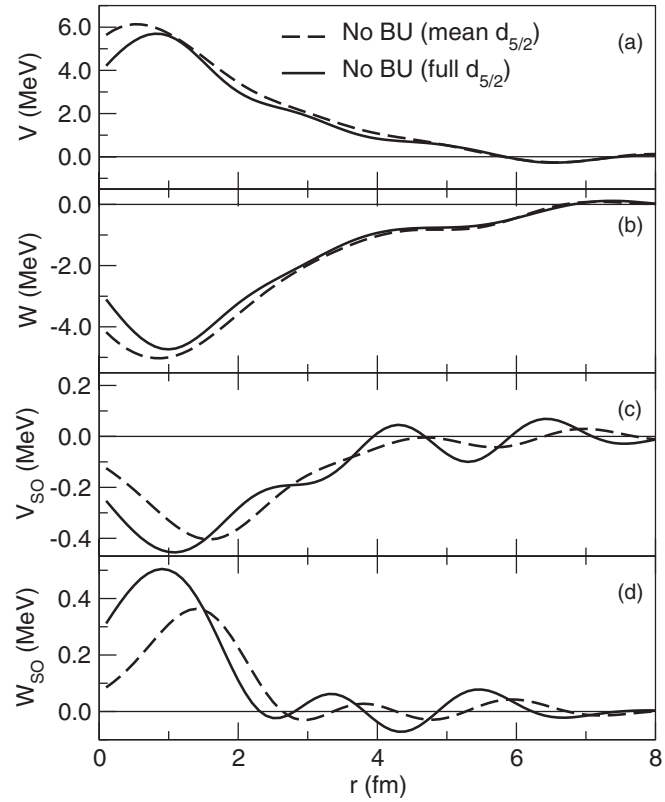

FIG. 3. For 30.3 MeV protons scattering from ^{40}Ca, the DPPs calculated by inversion and subtraction of the bare potential. The dashed lines are for the case "All $(3 \times 5/2^+)$" and the solid lines for the "All $(9\times 5/2^+)$" case. From top to bottom, we present the real (a) and imaginary (b) central DPPs, then the real (c) and imaginary (d) spin-orbit DPPs.

relates to the fact that the reaction coupling systematically increases the rms radius of the real potential, as can be seen from the $\Delta R_{\rm rms}$ values in Table I. Note also that the real-central potential in Fig. 3 shows attraction beyond 6 fm. This is not an artifact of the inversion procedure: inspection of the S matrix shows a coupling-induced increase in phase shift for $L \geqslant 10$.

Indications of nonlocality. The significance of the lines in Table I and elsewhere that present sums of specific contributions lies in the fact that the DPPs presented here are the local and L-independent equivalents (i.e., having the same S matrix) of the formal nonlocal and L-dependent DPPs. Since there is no coupling between the different deuteron channels, the formal DPPs corresponding to different states of ^{39}Ca must add to give the overall (nonlocal and L-dependent) DPP for that set of states. The differences between the "All $(3 \times 5/2^+)$" and "Sum" quantities in Table I therefore provide evidence for the nonlocality of the underlying DPPs. It is well-known that the local equivalent of the sum of nonlocal potentials is not the sum of the local equivalents of the individual potentials (see Ref. [2]).

Dependency relationships. The quantity $\Delta J_{\rm IM}$ is roughly proportional to Δ(Reac CS) with a weak dependence on the j transfer. For states in the order listed in Table I, the quantity $R_{\rm I}$ defined as

$$R_{\rm I} = \frac{\Delta J_{\rm IM}}{\Delta(\text{Reac CS})} \tag{1}$$

takes the values 0.28, 0.22, 0.26, 0.23, 0.26, and 0.20 (i.e., relatively constant over the range of $\Delta J_{\rm IM}$ values). By contrast, $\Delta J_{\rm R}$ varies from case to case in a very different way, and for the three $5/2^+$ states it is $R_{\rm R}$ defined through

$$R_{\rm R} = -\frac{\Delta J_{\rm R}}{[\Delta(\text{Reac CS})]^2}, \tag{2}$$

which is relatively constant, taking values 0.0022, 0.0032, and 0.0022, respectively, so that, for these three states of very different strengths, $\Delta J_{\rm R}$ is roughly proportional to $[\Delta(\text{Reac CS})]^2$. This, however, does not hold very closely for the other states, nor does it hold when, later, the spectroscopic factor is varied. The different behaviors of $R_{\rm I}$ and $R_{\rm R}$ appear to reflect a fundamental property of the DPP (see Sec. 2.9 of Ref. [11]).

It is interesting to compare Δ(Reac CS) (involving the total absorption CS) with the integrated CS calculated by FRESCO for the transfer states in question and presented in the last column

of Table I. The increase in reaction cross section induced by the coupling is much greater than the reaction cross section to the coupled states; it is as if the reaction channels are acting as a doorway to absorption and suggests an examination of the effect of modifying the imaginary part of the deuteron OMP. The $1/2^+$ state ($l = 0$ transfer) is associated with a lower ratio of Δ(Reac CS) to State CS than the higher l states. The effect of pickup is exactly the opposite of what is seen in the case of ^{6}Li scattering when breakup channels are included in a CDCC calculation; in that case [17], the increase in total cross section that is induced by breakup is several times *less* than the cross section into the breakup states.

Linearity test. Since the DPPs for the various cases to be described are all calculated using the same bare potential which, moreover, does not lead to a perfect fit to the AD and AP in the full CRC calculation, it is legitimate to ask whether the DPPs that we present are independent of reasonable adjustments to the bare potential. One approach to answering this is the linearity test, as follows: the DPP is subtracted from the bare potential $V_{\rm b}$ to produce a new bare potential $\bar{V}_{\rm b}$. The CRC calculation is then performed using $\bar{V}_{\rm b}$ as the bare potential, and S_{lj} is inverted to give V_2. If the system were perfectly linear, which would require the DPP to be independent of the bare potential, then $V_2 = V_{\rm b}$. The row "Linearity test" in Table I presents the characteristics of $V_2 - V_{\rm b}$ which can be seen to be small, especially for the central components. The linearity test employed the "All $(3 \times 5/2^+)$" set of pickup channels. We conclude that the general properties of the DPP deduced here are not strongly dependent on the particular bare potential chosen. Figure 2 demonstrates this linearity for the "All $(3 \times 5/2^+)$" set of states by comparing the AD and AP calculated in two ways. The solid line presents a one-channel calculation with the bare potential $V_{\rm b}$ of Hnizdo [15]. The dashed line presents the full CRC calculation with a new bare potential $\bar{V}_{\rm b} = V_{\rm b} - V_{\rm DPP}$ where $V_{\rm DPP}$ is the DPP calculated with the given set of states and the original bare potential $V_{\rm b}$. The agreement is good, consistent with the small values in the "Linearity test" line of the table. We remark that a necessary, although not sufficient, condition for the linearity we have demonstrated is the effectiveness of the $S_{lj} \rightarrow V$ inversion.

B. Tests with $3/2^+$ state

Why does pickup coupling (predominantly) lead to repulsion? In order to get some clues, we made a number of calculations to study the effects of different angular momentum transfer, different OMPs, the influence of deuteron breakup (BU), etc. In this section we compare DPPs due to coupling to just the $3/2^+$ ground state of ^{39}Ca when various parameters are modified. The results are presented in Table II.

$3/2^+$ with "stage-1" breakup of deuteron. For lighter target nuclei, it was found that the subsequent breakup of the deuteron substantially modified the pickup DPP [2–4]. Line "$3/2^+$ (BU 1st)" presents characteristics of the DPP for a calculation which includes breakup of the deuteron, calculated through the CDCC formalism. (It is designated "stage 1" because the computationally very demanding calculations to prove convergence of the breakup calculation have not been performed.) In this case the magnitudes of both $\Delta J_{\rm R}$ and $\Delta J_{\rm IM}$ are somewhat increased by the BU; for halo nuclei [2–4] the magnitude of $\Delta J_{\rm R}$ was reduced. All subsequent test calculations omit breakup of the deuteron.

Modifying the coupling strength. The "$3/2^+$ Sum rule" line in Table II gives the result of a calculation which repeats that of the first line except that the spectroscopic factor (SF) for the transfer to the $3/2^+$ g.s. of ^{39}Ca is increased to the value expected for a state that is a pure $3/2^+$ hole state. In the unmodified case "$3/2^+$," the SF was taken from our reanalysis [13] of the ^{40}Ca$(d,t)^{39}$Ca pickup data of Doll *et al.* [14]; this was then increased to the sum-rule value, giving a 1.674-fold increase in the spectroscopic factor. The volume integrals of the various components of the DPP increase by factors that are systematically greater than 1.674, markedly so for the spin-orbit components. We conclude that the characteristics of the

TABLE II. For protons scattering from ^{40}Ca at 30.3 MeV/nucleon, volume integrals ΔJ (in MeV fm^3) of the four components of the DPP induced by (p,d) coupling to the $3/2^+$ ground state of ^{39}Ca. The $3/2^+$ line is reproduced from Table I for convenience of comparison.

States coupled	$\Delta J_{\rm R}$	$\Delta J_{\rm IM}$	$\Delta J_{\rm RSO}$	$\Delta J_{\rm IMSO}$	$\Delta R_{\rm rms}$	Δ(Reac CS) (mb)	State CS (mb)
$3/2^+$	−12.53	14.64	0.8605	−0.3257	0.0344	52.47	7.93
$3/2^+$ (BU 1st)	−15.12	16.41	0.8275	−0.0341	0.0409	57.33	4.84
$3/2^+$ Sum rule	−23.66	30.55	2.1445	−1.623	0.0675	94.27	12.88
$3/2^+$ ($0.5 \times p$ imag)	−8.67	24.74	0.556	−0.407	0.0610	257.51	10.92
$3/2^+$ (zero proton imag)	−11.09	12.54	0.6945	−0.373	0.0275	219.26	16.767
$3/2^+$ (zero p,d imag)	−20.15	7.116	1.6475	0.3320	0.0572	155.0	155.0
$3/2^+$ ($1.2 \times d$ imag)	−11.01	13.95	0.758	−0.4074	0.0302	52.36	5.492
$3/2^+$ ($0.8 \times d$ imag)	−14.93	15.71	1.094	−0.248	0.0374	53.31	11.856
$3/2^+$ (d real $*0.8$)	+0.51	20.86	−0.6241	−1.888	0.101	75.47	13.69
$3/2^+$ (d real $*0.85$)	−3.68	21.51	0.1762	−1.8316	0.0236	76.27	14.05
$3/2^+$ (d real $*0.9$)	−7.73	20.24	0.7655	−1.2262	0.0327	71.36	12.82
$3/2^+$	−12.53	14.64	0.8605	−0.3257	0.0344	52.47	7.93
$3/2^+$ (d real $*1.1$)	−13.16	8.89	0.4360	0.1232	0.0215	32.48	3.49
$3/2^+$ (d real $*1.2$)	−11.39	4.89	0.1262	0.1113	0.010	18.83	1.406

DPP presented in the first line probably represent a lower limit to the contribution of $3/2^+$ states to the total potential. Noting that the factor by which the SF has been increased is the square of the factor by which the spectroscopic amplitudes were increased, these results remind us that the CC formalism includes coupling between incident and transfer channels to all orders. In spite of this, the State CS increased by a factor of 1.624, close to the increase in the SF.

For $3/2^+$ "sum-rule" calculations, from Eqs. (1) and (2) we find $R_I = 0.324$ and $R_R = 0.002\,66$; previously 0.280 and 0.0046, respectively. This follows an increase in almost all the listed quantities that is greater than the ratio of spectroscopic factors (spectroscopic amplitudes squared) of 1.674. Specifically, we see that

(i) ΔJ_R increased by factor 1.89;
(ii) ΔJ_{IM} increased by factor 2.09;
(iii) ΔJ_{RSO} increased by factor 2.49;
(iv) ΔJ_{IMSO} increased by factor 4.98;
(v) ΔR_{rms} increased by factor 1.96;
(vi) Δ(Reac CS) increased by factor 1.80;
(vii) State CS increased by factor 1.62.

The degree to which these ratios exceed 1.674 is evidence of the importance of higher-order contributions corresponding to more-than–second-order (p to d and back) coupling. The anomalously large increase in ΔJ_{IMSO} may be related to the fact that the form of the radial dependence suggests that the imaginary spin-orbit DPP is the result of canceling amplitudes. Note that the total cross section to the $3/2^+$ state increases by somewhat *less* than 1.674, but close enough that it is encouraging for the extraction of spectroscopic factors if it turns out to be a general result.

$3/2^+$ with the bare proton imaginary potential halved. It has been proposed (see, e.g., Ref. [18]), that the repulsive nature of the DPP is related to the imaginary part of the bare potential. In order to test this we performed calculations in which the imaginary component of the proton bare potential was reduced by a factor of 0.5. The results are presented in row "$3/2^+$ ($0.5 \times p$ imag)" where we see the magnitude of ΔJ_R is reduced and that of ΔJ_{IM} increased. In most cases, Δ(Reac CS) greatly exceeds the State CS, but in this case the difference is very large since the total reaction cross section is very small when there is no coupling. With coupling, the deuteron channels act as a doorway to absorption via the deuteron imaginary OMP. This is evident on the next line where the bare proton imaginary potential is set to zero so that almost all the reaction cross section must be due to the deuteron imaginary potential; it is clearly not in the outgoing deuteron flux.

$3/2^+$ with zero imaginary part in proton and deuteron channels. In the line "$3/2^+$ (zero p,d imag)" we show the characteristics of the DPP that arise when there is no absorption in either the bare proton OMP or outgoing deuteron potential. Thus, all of the reaction cross section corresponds to outgoing deuterons. There have been arguments that purely real propagating potentials should lead to an attractive real term in the DPP, but it is not necessarily so.

$3/2^+$ with 20% uniform increase in deuteron imaginary potential. In the line "$3/2^+$ ($1.2 \times d$-imag)" we present the effect of increasing the imaginary deuteron potential by a factor of 1.2. The line beneath, in which the imaginary deuteron potential is reduced with an overall factor of 0.8, reveals a linear response to this change. The magnitudes of ΔJ_R, ΔJ_{IM}, and the CS to the coupled state all increase as the absorption of the deuteron decreases, reflecting the increase in magnitude of the deuteron wave function. ΔJ_{IMSO} is an exception to the general increase in DPPs with decreasing deuteron absorption; as noted elsewhere this appears to involve interfering amplitudes.

$3/2^+$ with progressive modification of the deuteron real potential. The bottom section of Table II reveals a substantial sensitivity of the DPP to the depth of the real deuteron potential. The initial surprising result that a shallower deuteron potential led to *reduced* repulsion motivated this series in order to verify that the phenomenon was systematic and the first case studied was not an artifact. We do not understand these results; they, and the sensitivity to the imaginary deuteron potential, have the serious implication that a final evaluation of deuteron coupling effects must await the study of a case where (p,d) data are available.

C. Testing j dependence and Q dependence

In order to gain insight into the way in which the phenomenological optical potential might vary from nucleus to nucleus, and also to gain insight into the origin of the repulsive nature of the DPP, further model calculations were carried out.

TABLE III. For protons scattering from ^{40}Ca at 30.3 MeV/nucleon, volume integrals ΔJ (in MeV fm^3) of the four components of the DPP induced by (p,d) coupling. The $3/2^+$ line is reproduced from Table I for convenience of comparison.

States coupled	ΔJ_R	ΔJ_{IM}	ΔJ_{RSO}	ΔJ_{IMSO}	ΔR_{rms}	Δ(Reac CS) (mb)	State CS (mb)
$3/2^+$	−12.53	14.64	0.8605	−0.3257	0.0344	52.47	7.93
$5/2^+$ (like $3/2^+$)	−12.73	16.23	0.4497	0.8698	0.0298	53.69	7.70
$1/2^+$ (like $3/2^+$)	−16.11	15.82	0.4982	0.4665	0.0211	66.31	16.25
$1/2^+$ ($3/2^+$ SF)	−13.90	19.65	0.8115	0.3695	0.0306	77.67	17.98
$7/2^-$ (like $3/2^+$)	+2.49	16.46	1.3725	0.0461	0.0600	63.37	11.71
$7/2^-$ ($3/2^+$ SF)	+3.69	14.03	1.3465	−0.1698	−0.0042	57.53	7.82
$7/2^-$ (zero p,d imag)	+0.44	1.026	0.1681	0.0371	0.0026	23.0	23.0
$7/2^-$ (0. p,d imag, $Q = -8$)	−1.41	1.704	0.0520	0.1240	0.0037	35.4	35.4
$7/2^-$ ($Q = -8$)	−0.18	1.60	0.094	0.0529	0.0035	6.47	1.57

Table III presents results relating to the dependence of the DPP upon various parameters.

We first discuss the dependence of the spin-orbit DPP on the j transfer of the pickup transition. This is of interest because the way that the DPP depends upon the available neutron orbitals is relevant to explaining departures of optical model (OM) parameters from global behavior. One aspect of this is the dependence upon j transfer for a given l transfer. Comparing the DPPs for the two $l = 2$ states, referring back to Table I (comparing lines 1 and 3), we see specific differences in the spin-orbit (SO) terms. In particular, the imaginary SO term is negative for the $3/2^+$ state but positive for the 5.6175 MeV $5/2^+$ state. The real SO DPP is positive in both cases, but larger for the $3/2^+$ state than for the $5/2^+$ state; however, the overall DPP is larger for the $3/2^+$ state in this case and so we now address how much of the difference between the SO DPPs in lines 1 and 3 of Table I is a result of different Q values and spectroscopic factors.

Referring now to Table III, the line marked "$5/2^+$ (like $3/2^+$)" presents the characteristics of the DPP for pickup to a $5/2^+$ state having exactly the Q value and spectroscopic factor of the $3/2^+$ state. The central DPPs now have a similar magnitude to those for pickup to the $3/2^+$ state. The change in Q value and SF has a much greater effect on $\Delta J_{\rm R}$ than on $\Delta J_{\rm IM}$ and Δ(Reac CS), and this is reflected in the fact that $R_{\rm I} = 0.302$, see Eq. (1), and $R_{\rm R} = 0.00442$, see Eq. (2). These values are now close to those for the $3/2^+$ state: 0.280 and 0.0046, respectively. The SO terms are quite unlike those for $3/2^+$ transfer, with the real parts having different strengths and the imaginary parts having opposite signs. Examination of the radial dependence of the SO DPPs (not shown) reveals that, for the $5/2^+$ state, the imaginary part is absorptive for $r \leqslant 5$ fm while the real term tends to be repulsive within 3 fm and attractive outside 4 fm, with the attraction dominating the volume integral. The SO DPP generated by coupling to the $3/2^+$ state is quite different: the imaginary part is emissive for $r \leqslant 4$ fm whereas the real part is predominantly attractive, particularly for $r \leqslant 4$ fm. In summary: for $l = 2$, the change in j transfer has a small effect on the central DPP and a large effect on the SO DPP.

The l dependence was probed by evaluating the DPP for a "$1/2^+$ only" transfer in which the spectroscopic factor and Q value were the same as those for the "$3/2^+$ only" case. The characteristics are given in the "$1/2^+$ (like $3/2^+$)" line of Table III. For this case, $R_{\rm I} = 0.239$ and $R_{\rm R} = 0.00366$. Also in this case, a smaller l transfer leads to greater repulsion; $|\Delta J_{\rm R}|$ increases. This is consistent with $l = 3$ transfer for which there is attraction.

Line "$1/2^+$ ($3/2^+$ SF)" presents results for coupling to the $1/2^+$ state with the spectroscopic factor for the $3/2^+$ state but with the actual excitation energy so that the dependence upon the spectroscopic factor can be deduced independently of Q value; the comparison is with line 2 of Table I. The ratio of spectroscopic factors for the $3/2^+$ and $1/2^+$ states is 2.95, and this may be compared with the factors by which the real-central and imaginary-central DPPs increase for fixed Q value: $13.90/4.0 = 3.475$ and $19.54/5.62 = 3.496$, respectively. These both exceed 2.95, exhibiting the nonlinear response of all-order CRC. A comparison with the line above in this table reveals that the more negative Q value for pickup of the $1/2^+$ neutron (with the $3/2^+$ spectroscopic factor) reduces the magnitude of the real DPP and increases the imaginary DPP, as measured by the volume integrals.

We saw previously that coupling to the $7/2^-$ state state led to a small *attractive* real DPP; the only case of attraction. This is presumably connected with the greater l transfer. To verify this, we calculated the DPP for this case with the same Q value and spectroscopic factor as the $3/2^+$ state (line 1 of Table III). The results are in the line "$7/2^-$ (like $3/2^+$)" showing that there is indeed attraction, in this case enhanced by the larger SF.

In order to distinguish Q-value effects from the SF dependence, we present in the line "$7/2^-$ ($3/2^+$ SF)" results with the original $7/2^-$ Q value, but with the SF for the $3/2^+$ case. The ratio of spectroscopic factors was 11.95 whereas the factors by which the real-central and imaginary-central DPPs increased were rather less: 8.79 and 10.88, respectively; $\Delta J_{\rm IMSO}$ and $\Delta R_{\rm rms}$ change sign suggesting that interference between different amplitudes is involved. The difference between the "$7/2^-$ (like $3/2^+$)" and the "$7/2^-$ ($3/2^+$ SF)" cases is that the Q value of the latter is more negative by 2.796 MeV. This is sufficient to change the balance between real and imaginary DPPs as it did for the $1/2^+$ transfer.

It follows from the above that $l = 3$ transfer differs from $l = 0$ transfer in two respects: the real DPP is attractive instead of repulsive, and the DPPs vary with a lower power of the SF. Although the magnitude of the $l = 3$ DPPs depends upon Q value, the attractive character of $l = 3$ transfer does not.

$7/2^-$ state with zero imaginary part in proton and deuteron channels. In the line "$7/2^-$ (zero p,d imag)" we find that the DPPs, etc. are surprisingly close to those, in Table I, calculated with full imaginary potentials: the small attractive real-central term is remarkably close. The small increase in reaction cross section is, of course exactly equal to the cross section of the $7/2^-$ state, which is much greater than it was when the imaginary potentials were included. In the line below, "$7/2^-$ (0. p,d imag, $Q = -8$)," the same calculation is performed but with the binding energy of the $7/2^-$ state artificially reduced, changing the Q value for this state from -16.2126 to -8.0 MeV. Unsurprisingly, the magnitude of the DPPs increases but, notably, the sign of the real-central DPP changes, becoming repulsive. This dependence of the sign of the real-central DPP upon the energy of the outgoing deuteron might be a clue to understanding when and why repulsion emerges from pickup coupling. Remarkably, retaining $Q = -8.0$ MeV but restoring the standard absorption in proton and deuteron channels led to very small DPPs, with a tiny repulsive real-central term as in the line "$7/2^-$ ($Q = -8$)." The small repulsive real-central DPP may result from a transition from attractive to repulsive that occurs in this range of Q value.

D. Evaluating the need for higher-order terms

Valuable work has been done in deriving pickup contributions to the proton OMP based on the second-order distorted wave Born approximation (DWBA) using lowest-order Green functions (see, e.g., [19,20]). We shall, for brevity, refer to

these as UD ("up down") calculations. Such UD calculations can readily be made by a CRC code such as FRESCO by restricting the number of iterations, and they are very much quicker than fully converged all-order CRC calculations. Moreover, they can include nonorthogonality corrections and a full finite-range description of the pickup and stripping couplings. The great advantage in computing time would make possible extensive parameter searching that might be impractical for a full CRC calculation. UD calculations would also greatly speed up CRC calculations that include breakup of the outgoing deuteron; the importance of deuteron breakup for the DPP was indicated in Ref. [2] (see also Refs. [3,4]), and preliminary investigations suggest that it is important for both the magnitude and shape of the (p,d) angular distributions in the case of protons scattering from ^{40}Ca. It is also important for the DPP since the magnitude of the latter is sensitive to the spectroscopic factors that must ultimately be determined by the (p,d) fits. Determining the contribution of deuteron breakup to the pickup DPP would be greatly facilitated if this could reliably be determined in the context of UD calculations.

We are therefore motivated to evaluate UD calculations as an alternative to full CRC calculations of the DPP. We now present results of such calculations that, incidentally, lead to some further insights into coupled channel effects.

Coupling to the $3/2^+$ state. In Fig. 4 we compare the UD and full CRC DPPs generated by coupling to the $3/2^+$ state. The central terms in each case are similar at the surface, but that from the full CRC calculation is larger in magnitude for $r <$ 4 fm, slightly for the real term, but markedly for the imaginary term, and that is also true for the imaginary spin-orbit term. The fact that the real-central term is slightly smaller in magnitude between 4 and 6 fm for the full CRC case, together with the r^2 weighting in the volume integral, accounts for the fact that the real-central volume integral slightly increases in magnitude for the UD case in the comparison of lines 1 and 2 in Table IV, where we compare characteristics of the DPP for these and a number of other cases. Line 3 of Table IV presents the characteristics of the DPP for the UD calculation in which the spectroscopic factor is increased to the sum-rule strength. This amounts to multiplying the spectroscopic amplitude by 1.2940. The cross section leading to the $3/2^+$ state increases by exactly the square of this, 1.6744, as it must in a UD calculation. The underlying nonlocal and L-dependent DPP must also increase by that factor, but the local equivalent does not, as can be seen from line 3; for example $12.82 \times 1.6744 = 21.47$ and not 23.89. The numbers for the other quantities in line 2, multiplied by 1.6744, are given in line 4, from which it can be seen that the numbers in line 3 all depart from the linear response that might be expected, with the imaginary spin-orbit term even changing in sign. These differences are a consequence of the nonlocality of the underlying DPP, as would be calculated directly in the Green function formalism that was applied by Ref. [19]. This consequence of nonlocality is discussed in Ref. [2], and also by Franey and Ellis [21]. For convenience, line 5 repeats from Table II values for the $3/2^+$ transfer with sum-rule strength. It can be seen that the relationship between lines 5 and 3 bears a very similar relationship to that between lines 1 and 2, respectively. For the central potential, the effect of the higher-order processes is much greater for the imaginary part than for the real part: the higher-order terms substantially increase the absorption, and to a greater degree with the larger spectroscopic factor.

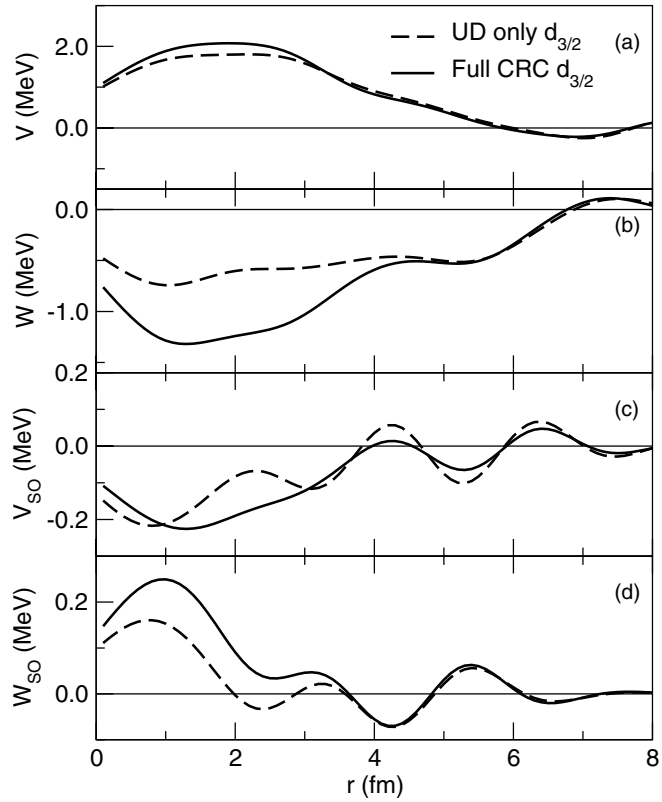

FIG. 4. For 30.3 MeV protons scattering from ^{40}Ca, the DPPs calculated by inversion and subtraction of the bare potential. The full lines are for the CRC calculation in which the $3/2^+$ ground state of ^{39}Ca is excited with a realistic spectroscopic factor, while the dashed lines are for the same reaction with lowest-order "UD" coupling. From top to bottom, we present the real (a) and imaginary (b) central DPPs, then the real (c) and imaginary (d) spin-orbit DPPs.

Comparing lines 1, 5, and 6 with lines 2, 3, and 4 reveals that the nonlinear response of the DPPs to changes in the spectroscopic factor for the full CRC calculation is greater than for the UD calculation. The ratios implicit in line 5 were given in Sec. III B; it was suggested that the large ratio for $\Delta J_{\rm IMSO}$, 4.98, for the $3/2^+$ state was an indication of processes with interfering amplitudes; this appears to be true also in the UD case.

The relatively small effect of higher-order terms on the real-central DPP, as shown in Fig. 4, is consistent with the fact that the departure from a linear response of $\Delta J_{\rm R}$ to changes in the spectroscopic factor is almost the same for the UD and CRC calculations. This suggests that the nonlinearity in the CRC case is largely due to the nonlocality of the DPP as it must be in the UD case.

We note that the change in reaction cross section due to pickup coupling greatly exceeds the integrated cross section to the pickup state for UD and full CRC calculations alike.

As noted in the introduction, a motivation for CRC studies of proton scattering is the study of shell corrections to global nucleon potentials. This has been addressed

TABLE IV. For protons scattering from ^{40}Ca at 30.3 MeV/nucleon, volume integrals ΔJ (in MeV fm^3) of the four components of the DPP induced by (p,d) coupling. The $\Delta R_{\rm rms}$ column gives the change of rms radius of the real-central component (in fm). The two final columns present, respectively, the change in the total reaction cross section induced by the coupling, and the integrated cross section to the specific coupled reaction channels. Line numbers are referred to in the text.

States coupled	$\Delta J_{\rm R}$	$\Delta J_{\rm IM}$	$\Delta J_{\rm RSO}$	$\Delta J_{\rm IMSO}$	$\Delta R_{\rm rms}$	Δ(Reac CS) (mb)	State CS (mb)	Line
$3/2^+$	−12.53	14.64	0.8605	−0.3257	0.0344	52.47	7.93	1
$3/2^+$ UD	−12.82	11.97	0.6509	−0.0324	0.0314	41.35	8.0542	2
$3/2^+$ UD, sum rule	−23.89	19.69	1.1855	0.1145	0.0522	60.67	13.486	3
$3/2^+$ UD, ×1.6744	−21.47	20.04	1.0899	−0.0543	0.0526	69.24	13.486	4
$3/2^+$ sum rule	−23.66	30.55	2.1445	−1.6233	0.0675	94.27	12.88	5
$3/2^+$ ×1.6744	−20.98	24.51	1.4408	−0.5454	0.0576	87.86	13.28	6
$1/2^+$	−4.00	5.62	0.2224	0.0894	0.0088	25.77	6.51	7
$1/2^+$ UD	−4.11	5.24	0.2080	0.0935	0.0083	23.92	6.6234	8
$1/2^+$ UD, sum rule	−11.6	12.86	0.5013	0.2887	0.0212	53.05	16.332	9
$1/2^+$UD × 2.4658	−10.13	12.92	0.5130	0.2306	0.0205	58.98	16.332	10
$1/2^+$ sum rule	−11.19	15.55	0.6270	0.2718	0.0231	64.54	15.376	11
$1/2^+$ × 2.4658	−9.86	13.86	0.5484	0.2204	0.0217	63.54	16.05	12
All (3 × $5/2^+$)UD	−20.49	19.54	1.0045	0.1247	0.0425	65.91	17.807	13

phenomenologically [10]. In particular, the shell dependence of the spin-orbit interaction has been studied using UD calculations [19]. It is therefore relevant that the spin-orbit volume integrals for the $3/2^+$ case are quite sensitive to whether the UD approximation is made.

Coupling to the $1/2^+$ state. It is of interest to evaluate the importance of higher-order coupling to a state that is intrinsically weaker and that has a lower l transfer. Accordingly, the lower half of Table IV presents the characteristics of the DPP arising from the coupling to the $1/2^+$ state, including, for ease of comparison, the full CRC values in line 7. From line 8 we see that all quantities change following the same pattern as that seen between lines 1 and 2, with even the imaginary spin-orbit term increasing in the positive direction although the sign is different. As previously remarked, the changes to this term appear to be the result of interference between different processes. The percent changes in the quantities $\Delta J_{\rm IM}$, $\Delta J_{\rm RSO}$, $\Delta J_{\rm IMSO}$, $\Delta R_{\rm rms}$ and Δ(Reac CS) are all much greater for the $3/2^+$ state than for the $1/2^+$ state.

The sum-rule spectroscopic factor for the $1/2^+$ transfer is a factor of 2.4658 times greater than that leading to the values in lines 7 and 8. The state CS must increase by that factor and, indeed, $2.4658 \times 6.6234 = 16.332$. The other characteristics of the DPP would increase by the same factor if it were not for the nonlocality of the formal DPP and the nonlinearity of the process leading to the local equivalent DPP. This difference is evident from a comparison of lines 9 and 10. These differences are only roughly comparable to those between lines 3 and 4.

Common features of $3/2^+$ and $1/2^+$ coupling. There is some regularity in the response of the volume integrals of the DPPs to the change in magnitude of the spectroscopic factors: In both UD cases, the ratio of $\Delta J_{\rm IM}$ values is very close to the ratio of sum rule to standard spectroscopic factors, but the ratio of the $\Delta J_{\rm R}$ values is much larger, and to a similar degree in each case: ≈1.13× the ratio of the spectroscopic factors.

The ratios of $\Delta J_{\rm IM}$ standard and sum-rule values are similar for the two states. For $1/2^+$, they are 2.767 (CRC) and 2.45 (UD), compared with 2.4658. For $3/2^+$, they are 2.087 (CRC) and 1.645 (UD) compared with 1.6744. For both cases, the UD approximation fixes the increase in $\Delta J_{\rm IM}$ at the ratio of spectroscopic factors, which is not true for CRC.

By contrast, the ratios of $\Delta J_{\rm R}$ values are almost the same for CRC and UD and close to the ratios of spectroscopic factors: for $1/2^+$ the ratios are 2.797 (CRC) and 2.822 (UD) compared to 2.4658; for $3/2^+$ the ratios are 1.888 (CRC) and 1.863 (UD) compared to 1.6744. That is, for $\Delta J_{\rm R}$, the UD approximation makes no difference and the ratios exceed the ratio of spectroscopic factors by very similar factors.

The complete calculation. We have compared CRC and UD calculations for the complete calculation, as in the "All (3 × $5/2^+$)" line of Table I, and the results are in line 13 of Table IV. As in the other cases, the effect on the real-central volume integral is small, but the absorption is reduced, and the spin-orbit terms are changed. The corresponding AD and AP are given as dotted lines in Fig. 1 in which the effect on the AP appears to be greater than the effect on the AD.

Summary of UD versus CRC. The impact of the UD approximation is much greater on the imaginary-central term than on the real-central term. For the $3/2^+$ state, but not the $1/2^+$ state, the UD approximation has a significant impact on the spin-orbit DPP. For both UD and CRC and all components, the DPPs vary more rapidly than the spectroscopic factors. In both UD cases, as in all CRC cases, the increase in the total reaction cross section greatly exceeds the integrated cross section to the transfer state. In the UD calculations the cross section to the transfer state is directly proportional, as it must be, to the spectroscopic factor when that alone is changed. As a result of the nonlocality of the underlying DPP, the quantitative characteristics of the DPP are not proportional to the spectroscopic factor although this proportionality must hold for the underlying nonlocal and L-dependent DPP in UD calculations.

IV. SUMMARY AND CONCLUSIONS

A. Summary of findings

The real and imaginary central terms of the DPP for protons scattering from the ^{40}Ca nucleus are repulsive (except in the case of coupling to the $7/2^-$ state) and absorptive, respectively. The same repulsive-absorptive character had been found [2–4] for protons scattering from the untypical light nuclei ^{6}He and ^{8}He. For both these latter cases and for ^{40}Ca, the real-central DPP cannot be represented as a uniform renormalization of the bare potential since the real DPP tends to peak at the nuclear center in this case. This radial shape for the real-central DPP results in an increase of the rms radius of the total potential, whereas, for scattering from the halo nuclei ^{6}He [3] and ^{8}He [2,4], the shape of the repulsive DPP is such to decrease the rms radius. This difference currently remains a challenge to the understanding.

The repulsive DPP is smaller in magnitude than that previously studied [18] with a zero-range or adiabatic model coupling and no nonorthogonality correction. Subsequent calculations [22,23] with finite-range coupling but no nonorthogonality corrections also seem to lead to DPPs that are too large. The explicit evaluation of the contribution of nonorthogonality corrections was presented in Ref. [24], and it is clear that they must be included in studies of this kind.

The real and imaginary-central components of the DPPs (as measured by volume integrals) are proportional to different powers of the change in reaction CS (Eqs. (1) and (2).) The complete DPP depends upon the angular momentum of the transferred neutron in two ways: (i) for 30.3 MeV protons on ^{40}Ca, the repulsion appears to be greatest for lower orbital angular momentum transfer, actually becoming attractive for the weakly excited $l = 3$, $7/2^-$ state; and (ii) the imaginary spin-orbit DPP appears to have opposite signs for the single $3/2^+$ and the $5/2^+$ states, although the situation is unclear when several states are excited, and there are indications that, in this case, there are interfering amplitudes. The imaginary spin-orbit DPP appears to be small for the $1/2^+$ state. The Q value and l and j dependencies of the DPP should hopefully lead eventually to a way of correcting global OMPs to fit sequences of nuclei.

The accurate calculation of the DPP requires higher-order terms beyond second-order DWBA (the "up-down, or UD, approximation") as is most evident in the imaginary terms. All components depart from a linear dependence on the spectroscopic factor. For the real components, this departure is almost as great for UD calculations as for the full CRC calculations. The deviation of the UD DPP from a linear dependence upon the spectroscopic factor is a result of the nonlinearity implicit in the derivation of a local equivalent to the underlying nonlocal and L-dependent DPP. This underlying nonlocal DPP must depend linearly on the spectroscopic factor for the UD case.

The importance of including the breakup of the deuteron appears to be rather less for the ^{40}Ca target than for pickup from the light halo nuclei and has not been included in most of the specific test calculations described here. The great saving in computational time for the UD calculations when breakup is included should facilitate a further study of this.

We have presented evidence that the nonlocality arising from the pickup coupling is significant. This raises basic questions such as: Is the OMP that fits elastic scattering immediately appropriate for applying to transfer and other reactions? It is (or should be) standard practice to correct for the Perey effect [7] arising from the phenomenological representation of (and presumed actual) knock-on exchange. However, there is as yet no known simple means of correcting for the nonlocality arising from reaction channel coupling, and this requires study.

B. What does it all mean?

In Ref. [17] an explanation was proposed for the strong surface repulsion that is generated by the breakup of composite nuclear projectiles. It might be thought that similar arguments apply to the systematic repulsive effect of pickup-channel coupling. Earlier studies of this (e.g., Ref. [18]) suggested that a connection with absorption in the coupled channel was involved; the fact that attractive DPPs occur when the potentials in the coupled channel are real [25] seems to support this. However, the calculations described here do not give unambiguous support to various hypotheses that have been proposed and the complexity of the situation can be seen in evidence in Table II that, (i) increasing the absorption in the deuteron channel decreases the repulsive effect and, (ii) deepening the real deuteron potential (generally) increases the repulsion. It would appear that momentum and angular momentum transfer as well as the absorption of the projectiles all play a role.

An understanding of the nature of these processes that contribute to the nucleon-nucleus interaction is highly desirable, and coupled channel calculations rather than Green function methods are, for reasons discussed in Ref. [2], the appropriate means of including the full complexity (finite range, deuteron D state, nonorthogonality corrections) of transfer reactions together with the propagation of the projectiles in the strong gradient curved surface nuclear field. In this work, we have demonstrated how easy and reliable it is to extract local equivalent DPPs using IP inversion. A necessary, although not sufficient, condition for the linearity presented in Table I is the accuracy of IP inversion.

It is our view that further work in this direction should be for a case where good (p,d) data exists so that we can ensure that both the spectroscopic factors and the deuteron optical potential are appropriately optimized. Note that the determination of the spectroscopic factor is nontrivial in view of the limitations of the UD approximation of Sec. III D. This is the beginning, not the end, of studies of CRC effects on elastic nucleon scattering on heavier targets. The present work does not solve the problem of how to fit the backward angle AD and AP for 30.3 MeV scattering of protons from ^{40}Ca. To date, these data have been fit only with nonstandard phenomenology: either L-dependent potentials [26,27] or somewhat wavy potentials found by spline fitting [28]. Whether these data can be fit with a smooth potential plus CRC coupling to pickup channels is a challenge for the future.

The evidence we have presented of nonlocality, and presumably L dependence, reflects the fact that we are studying effects that go beyond any local density model in which the OMP is derived from just the nuclear density $\rho(r)$. We take into account both the specific occupied orbitals and available reaction channels, but also the propagation of the coupled nuclei (deuterons in this case) in the density gradients of the nucleus. This is the way in which angular momentum dependence and nonlocality are introduced, as they are more formally in the Feshbach theory.

There remains the question of how the reaction coupling effects can be accommodated with the highly developed folding models such as those of Refs. [29,30]. At the phenomenological level, it would be interesting to find, by means of model-independent fitting, the various terms that would, when added to such theoretical potentials, yield perfect fits to the data, thus exploiting all the information contained in the data sets for certain cases. This is arguably much sounder than searching for normalization factors for the various components; such restricted fits are unlikely to fit the data precisely. It would, of course, be particularly interesting if the model-independent addition yielded functional forms resembling the radial forms of the DPPs found in the present work.

ACKNOWLEDGMENTS

R.S.M. is grateful to Daisy Hirata for computational assistance.

[1] R. S. Mackintosh and N. Keeley, Phys. Rev. C **76**, 024601 (2007).
[2] R. S. Mackintosh and N. Keeley, Phys. Rev. C **81**, 034612 (2010).
[3] N. Keeley and R. S. Mackintosh, Phys. Rev. C **83**, 044608 (2011).
[4] R. S. Mackintosh and N. Keeley, Phys. Rev. C **83**, 057601 (2011).
[5] V. I. Kukulin and R. S. Mackintosh, J. Phys. G: Nucl. Part. Phys. **30**, R1 (2004).
[6] R. S. Mackintosh, arXiv:1205.0468.
[7] F. G. Perey, *Direct Interactions and Nuclear Reaction Mechanisms*, edited by E. Clemental and C. Villi (Gordon and Breach, New York, 1963), p. 125.
[8] N. Austern, Phys. Rev. B **137**, 752 (1965).
[9] R. S. Mackintosh and S. G. Cooper, J. Phys. G: Nucl. Part. Phys. **23**, 565 (1997).
[10] H. Sakaguchi, M. Nakamura, K. Hatanaka, T. Noro, F. Ohtani, H. Sakamoto, H. Ogawa, and S. Kobayashi, Phys. Lett. B **99**, 92 (1981).
[11] G. R. Satchler, *Direct Nuclear Reactions* (Clarendon Press, Oxford, 1983).
[12] I. J. Thompson, Comput. Phys. Rep. **7**, 167 (1988).
[13] N. Keeley and R. S. Mackintosh, Phys. Rev. C **77**, 054603 (2008).
[14] P. Doll, G. J. Wagner, K. T. Knopfle, and G. Mairle, Nucl. Phys. A **263**, 210 (1976).
[15] V. Hnizdo, O. Karban, J. Lowe, G. W. Greenlees, and W. Makofske, Phys. Rev. C **3**, 1560 (1971).
[16] A. J. Koning and J. P. Delaroche, Nucl. Phys. A **713**, 231 (2003).
[17] D. Y. Pang and R. S. Mackintosh, Phys. Rev. C **84**, 064611 (2011).
[18] R. S. Mackintosh, Nucl. Phys. A **230**, 195 (1974).
[19] S. Kosugi and Y. Yoshida, Phys. Lett. B **106**, 353 (1981).
[20] S. Kosugi and Y. Yoshida, Nucl. Phys. A **373**, 349 (1981).
[21] M. A. Franey and P. J. Ellis, Phys. Rev. C **23**, 787 (1981).
[22] R. S. Mackintosh, A. A. Ioannides, and I. J. Thompson, Phys. Lett. B **178**, 1 (1986).
[23] S. G. Cooper, R. S. Mackintosh, and A. A. Ioannides, Nucl. Phys. A **472**, 101 (1987).
[24] F. Skaza *et al.*, Phys. Lett. B **619**, 82 (2005).
[25] C. L. Rao, M. Reeves, and G. R. Satchler, Nucl. Phys. A **207**, 182 (1973).
[26] A. M. Kobos and R. S. Mackintosh, J. Phys. G: Nucl. Phys. **5**, 97 (1979).
[27] A. M. Kobos and R. S. Mackintosh, Acta Physica Polonica B **12**, 1029 (1981).
[28] A. M. Kobos and R. S. Mackintosh, Ann. Phys. (NY) **123**, 296 (1979).
[29] E. Bauge, J. P. Delaroche, and M. Girod, Phys. Rev. C **63**, 024607 (2001).
[30] H. F. Arellano and E. Bauge, Phys. Rev. C **84**, 034606 (2011).